9276–9290 *Nucleic Acids Research, 2015, Vol. 43, No. 19* *Published online 14 August 2015*
doi: 10.1093/nar/gkv817

Mapping the interactions of the single-stranded DNA binding protein of bacteriophage T4 (gp32) with DNA lattices at single nucleotide resolution: gp32 monomer binding

Davis Jose, Steven E. Weitzel, Walter A. Baase and Peter H. von Hippel*

Institute of Molecular Biology and Department of Chemistry, University of Oregon, Eugene, OR 97403-1229, USA

Received March 14, 2015; Revised July 13, 2015; Accepted July 31, 2015

ABSTRACT

Combining biophysical measurements on T4 bacteriophage replication complexes with detailed structural information can illuminate the molecular mechanisms of these 'macromolecular machines'. Here we use the low energy circular dichroism (CD) and fluorescent properties of site-specifically introduced base analogues to map and quantify the equilibrium binding interactions of short (8 nts) ssDNA oligomers with gp32 monomers at single nucleotide resolution. We show that single gp32 molecules interact most directly and specifically near the 3′-end of these ssDNA oligomers, thus defining the polarity of gp32 binding with respect to the ssDNA lattice, and that only 2–3 nts are directly involved in this tight binding interaction. The loss of exciton coupling in the CD spectra of dimer 2-AP (2-aminopurine) probes at various positions in the ssDNA constructs, together with increases in fluorescence intensity, suggest that gp32 binding directly extends the sugar-phosphate backbone of this ssDNA oligomer, particularly at the 3′-end and facilitates base unstacking along the entire 8-mer lattice. These results provide a model (and 'DNA map') for the isolated gp32 binding to ssDNA targets, which serves as the nucleation step for the cooperative binding that occurs at transiently exposed ssDNA sequences within the functioning T4 DNA replication complex.

INTRODUCTION

The DNA replication system of the T4 bacteriophage resembles those of higher organisms in both its protein composition and functional sub-assemblies, and thus can serve as a useful model for the central features of these complex 'macromolecular machines' (1–4). As in higher organisms, the T4-coded replication complex consists of three sub-assemblies (the DNA polymerases, the helicase-primase-containing primosome and the processivity clamp-clamp loader), which are separately stable and functional and can be reconstituted from their protein subunit components and studied *in vitro* (3–5). Gene 32 protein (gp32), the single-stranded DNA binding (ssb) protein of the T4 replication complex, plays a central integrating role in the functioning of the many components of the T4-coded replication and recombination complexes. Moreover its intrinsic interactions with the ssDNA lattice in both the isolated and cooperative binding modes are presumed to be central to its function, and these interactions can be studied separately (6).

Gp32 binds transiently and cooperatively to ssDNA template sequences as these entities are exposed by the processive primosome helicase operating within the replication complex and this binding puts these ssDNA sequences into optimal conformations for interacting with DNA polymerases and other replication proteins. By coating these transiently exposed ssDNA sequences, gp32 also protects them from degradation by nucleases while they discharge their templating (and other) functions in association with the leading- and lagging-strand DNA polymerases. In addition, the formation of a ssDNA filament coated with gp32 is an early step in genetic recombination (7). After all the ssDNA within the replication complex has been complexed, additional gp32 binds to a long (∼9 gp32 monomer binding sites at saturation) unstructured sequence on the mRNA coding for the gp32 gene, thereby autogenously regulating the synthesis and thus the concentration of this protein in the Escherichia *coli* host cell during the replication process (8).

The gene 32 protein of bacteriophage T4 (together with its *E. coli*-coded analog, which shows somewhat different cooperativity behavior (9)) is probably the most widely studied and best understood member of the ssb protein class, and biochemical insights obtained from studies of gp32 continue to serve as an important basis for understanding the function of these proteins in bacteria and higher organ-

*To whom correspondence should be addressed. Tel: +1 541 346 5151; Fax: +1 541 346 5891; Email: petevh@molbio.uoregon.edu

isms. Gp32 interacts with other components of the replication complex during the DNA replication cycle, and in the course of these interactions it must transiently bind and unbind (initially as isolated monomer subunits and then cooperatively) ssDNA sequences in response to the requirements of the other components of the replication complex as they manipulate the genomic DNA. In addition, short contiguously bound 'blocks' of gp32 likely 'slide' or 'hop' along the ssDNA to permit stoichiometric coating of the ssDNA sequences. To discharge these multiple functions, a variety of interactions of the gp32 with its substrate DNA are required and our purpose in this study is to seek a greater understanding of these interactions by mapping the binding interactions of both isolated and cooperatively-bound gp32 protein with its ssDNA targets at single nucleotide residue (nt) resolution.

Gene 32 protein in solution in the absence of DNA binding targets exists primarily as protein monomers (10). The 'core' or central portion of the gp32 monomer (from which the N- and C-terminal regulatory domains can be removed by limited tryptic digestion) is the ssDNA-binding domain and comprises 235 amino acid residues. This core domain contains an oligonucleotide-oligosaccharide binding fold (OB-fold)—a motif generally found in ssDNA binding proteins—and confers ssDNA binding specificity and polarity (11) onto the gp32 molecule. A crystal structure of the gp32 core bound to a short ssDNA oligomer has been reported (12). The N-terminal (20 amino acid residues) domain of the gp32 protein is required for the cooperative binding of gp32 monomers to long ssDNA lattices and the C-terminal domain (46 residues) is essential for the regulatory interactions of gp32 with other proteins of the T4-coded DNA replication, recombination and repair complexes (13,14).

Thermodynamic parameters characterizing gp32 binding to DNA (and RNA) have been measured by monitoring changes in the intensity of the intrinsic protein fluorescence that accompany binding (14–17). More recently parameters derived from extrapolating single molecule force ('pulling') measurements to equilibrium conditions have also been used to confirm thermodynamic parameters measured in bulk solution, while the non-equilibrium force-extension curves obtained in these experiments have provided insights into kinetic issues, including some aspects of the molecular basis of binding cooperativity and the 'kinetic block' that prevents gp32 from irreversibly 'melting' the duplex DNA of the genome (18–21). Early studies showed that the 'occlusion' binding site size (n) for gene 32 monomers to ssDNA is 7 nt, and the existence of long-range binding cooperativity, required for lattice saturation, suggested that binding must be head-to-tail (and thus polar) along the ssDNA chain (the 'occlusion' site-size defines the number of contiguous nucleotide residues (nts) 'covered' (i.e. rendered unavailable to another binding ligand) per bound gp32 monomer in cooperative ssDNA or ssRNA binding. In contrast the 'interaction' site size defines the number of contiguous (or non-contiguous) nts that interact directly with each gp32 molecule and thus contribute directly to the gp32–ssDNA binding free energy ($\Delta G_{ssDNA\text{-}bind}$).) Gp32 binds to single-stranded nucleic acid lattices in different modes, depending both on lattice length and binding density (22,23). Lattices 2–8 nts in length are bound in an 'isolated' mode, which differs significantly from the 'cooperative' binding mode characteristic of longer lattices at high binding densities.

The observed association constant for the binding of isolated gp32 molecules to short DNA lattices (K_{assoc}) is $\sim 10^5$ M^{-1}, and the binding affinity of these short oligomers for gp32 is relatively independent of sugar type, base composition and salt concentration. The cooperative binding affinity per protein monomer for longer lattices is defined as $K\omega$, where K is the binding constant for each gp32 monomer to the lattice and ω is the cooperativity parameter for a contiguous binding interaction (24). The value of the $K\omega$ product is somewhat dependent on lattice sugar type and base composition, and also on salt concentration, although the dependence on these variables seems to reflect primarily changes in the value of K rather than of ω, at least at monovalent salt concentrations <0.2 M. The measured value of the cooperative binding constant ($K\omega$) is $\sim 10^8$ M^{-1} at physiological salt concentrations, with ω contributing about 10^3 (15). The binding of the protein to the lattice is quite different in the isolated and in the cooperative binding modes, and detailed studies of the reaction have led to (schematic) models that have been described in detail previously (13–15,21) and are further considered in the 'Discussion' section and in the companion paper (25). Consistent with known translational regulation mechanisms (15), cooperative binding ($K\omega$) of gp32 is stronger to ssDNA than to ssRNA, while binding of gp32 to dsDNA is essentially non-cooperative and somewhat weaker than isolated binding to either ssDNA or ssRNA [see (14,15) and references therein].

Gp32–DNA complexes have proven difficult to crystallize and thus have been structurally characterized to only a limited extent. An x-ray structure of the core protein domain (residues 21–254) of gp32, co-crystallized with a bound $(dT)_6$ oligomer, has been published (12). The putative binding cleft for ssDNA in this structure runs through a strongly electropositive region of the protein. It has been suggested (14) that, when ssDNA is *not* bound, three negatively charged residues of the C-terminal domain interact with positively charged residues located within this cleft and that ssDNA binding competes with and displaces the C-terminal domain from the binding cleft. We note that, although the core protein domain was co-crystalized with $(dT)_6$, only weak electron densities were observed for the ssDNA oligomer within the crystal structure of the complex and it proved impossible to resolve the ssDNA chain. However, Shamoo *et al*. did use the electron density attributable to the $(dT)_6$ oligomer to model a part of the $(dT)_6$ chain into the gp32 core domain structure, and their results suggested that at least two of the nucleotide residues at one end of the ssDNA oligomer might be tightly bound to the gp32 core. This conclusion is consistent with thermodynamic measurements of gp32 monomer binding, which showed that oligonucleotides between 2 and 8 residues in length displayed approximately equal binding affinities for gp32 monomers (15). These results suggested a possible structural basis for the polar binding of gp32 to ssDNA (or ssRNA) lattices, which our present results have strengthened and extended.

Significant changes in the salt-concentration-dependence of binding were observed for the reaction of gp32 protein with longer polynucleotides. However, this was not the case for the binding of short oligomers to the gp32 monomer (14) and aspects of the relationship of the cooperative binding mode of gp32 to the observed gp32 core domain-short oligonucleotide structure (11) remain unclear. Furthermore, the protein–protein and protein–DNA interactions within the complex, as well as the conformations of the components of the complex, may be expected to change as the gp32 protein switches from the isolated to the cooperative binding mode, 'slides' or 'hops' along the ssDNA lattice, interacts with other proteins of the replication complex or dissociates from ssDNA—all processes that are likely to occur during biological function. Thus there is a clear need for more information about the relation between the structure and dynamics of ssDNA binding and gp32 function.

Electron microscopy has shown that cooperative binding of gp32 to a ssDNA lattice significantly extends the sugar-phosphate backbone of the ssDNA (26,27). The limited x-ray crystallographic results with the gp32 monomer core domain also suggested that the ssDNA backbone might be extended as a consequence of oligonucleotide binding to the electropositive cleft of gp32 (12). General principles—for example, the requirement for cooperative binding to assure lattice saturation (24)—together with intrinsic protein fluorescence quenching measurements (22,28) suggested that the binding of gp32 must be polar (i.e. head-to-tail), but these bulk studies did not define the direction of the binding polarity relative to the sugar-phosphate backbone of the oligonucleotide target. This represents a significant unanswered question, because this isolated polar binding interaction doubtless serves as the nucleation step for cooperative gp32 binding to the ssDNA sequences transiently-exposed at the replication fork. Thus the establishment of these initial binding mechanisms is likely to be central to elucidating the molecular mechanisms of the cooperative binding and unbinding of gp32 and other ssDNA (or ssRNA) binding proteins during the replication process.

We have used the spectral properties of site-specifically positioned fluorescent analogs of the canonical bases as probes to study local conformational changes occurring at specific sites in a nucleic acid lattice (29,30), or at specific base positions in a protein-binding nucleic acid scaffold (31,32). The incorporation of these base analogs generally does not significantly alter the structural or biological properties of the nucleic acid lattice (29,30). Here we monitor the circular dichroism (CD) and fluorescent intensity changes of site-specifically positioned 2-aminopurine (2-AP) dimer probes to elucidate structural details of monomeric gp32 binding to short oligonucleotides. These results are then extended to provide structural interpretations of the cooperative binding mechanism in the companion paper (25).

MATERIALS AND METHODS

DNA constructs and buffers

Unlabeled and 2-AP-labeled DNA oligonucleotides were purchased from Integrated DNA Technologies (Coralville, IA, USA). DNA concentrations were determined by UV absorbance at 260 nm, based on extinction coefficients furnished by the manufacturer. The sequences and nomenclature of the DNA constructs used in this study are shown and described in Table 1. Unless stated otherwise, all experiments were performed at 20°C in buffer containing 10 mM HEPES (pH 7.5) and 30 mM potassium acetate (KOAc).

Table 1. Nomenclature and sequences of the DNA constructs

Construct	Sequence[a]
$d(T)_8$	5′ d(TTT TTT TT) 3′
${}_8P_{2,3}$	5′ d(Taa TTT TT) 3′
${}_8P_{4,5}$	5′ d(TTT aaT TT) 3′
${}_8P_{6,7}$	5′ d(TTT TTa aT) 3′
${}_8A_{2,3}$	5′ d(Aaa AAA AA) 3′
${}_8A_{6,7}$	5′ d(AAA AAa aA) 3′

[a]'T' represents Thymine, 'A' is Adenine and 'a' is the 2-AP probe(s). The subscripts before the construct names indicate the total length of the ssDNA lattice, and the subscripts that follow the names denote the positions of the probes within each construct.

Cell growth and protein purification

pYS6/AR120 cells (12) were grown to an optical density (OD_{600}) of 0.9 to 1.0 at 37°C in Luria-Bertani liquid medium (LB broth) containing 50μg/ml ampicillin. The cells were then induced by adding nalidixic acid to a final concentration of 40μg/ml, grown for an additional 8–10 h at 37°C and harvested. The gp32 protein was purified according to the procedure of Bittner *et al.* (33) and stored at −20°C in storage buffer containing 20 mM Tris–OAc (pH 8.1), 0.5 mM DTT, 1 mM EDTA, 50 mM KOAc and 50% glycerol. Stock solutions of the protein were dialyzed extensively against reaction buffer prior to each experiment.

Spectroscopic procedures

CD spectra were measured in 1 cm path-length cells at wavelengths from 300 to 400 nm using a JASCO model J-720 CD spectrometer equipped with a PTC-348W temperature-controlled sample holder. About10–15 spectra were scanned, averaged and plotted as graphs of $\Delta\epsilon$/AP, (where $\Delta\epsilon = \epsilon_l - \epsilon_r$, the difference in the molar extinction coefficient for left and right circularly polarized light per mol of 2-AP residue) as a function of wavelength. Fluorescence measurements were performed in a 4 × 4 mm rectangular cell in a Horiba FluoroMax 3 spectrophotometer. ssDNA constructs were manually titrated with successive aliquots of bacteriophage T4 gene 32 protein (gp32) at 20°C. The samples were gently mixed for 2 min at each gp32 concentration and then fluorescence emission intensities at 370 nm were collected using an excitation wavelength of 315 nm. Raw data were corrected for dark counts and for Raman scattering. A correction for background fluorescence was made by subtracting the fluorescence intensities obtained with an unlabeled ssDNA strand $d(T)_8$ following titration with the same amounts of gp32 as used in the experiment. The total concentrations of ssDNA oligomer and gp32 were calculated from the added volumes and the fluorescence data were fit to a quadratic 2-state binding equation to compute the concentration of 1:1 complex, as well as the fluorescence intensity of the complex.

The binding constant, K_b (per molar), and the fluorescence intensity (cps per molar) of the bimolecular complex, $F_{complex}$, were determined by iteratively fitting titration data in Origin 7 (OriginLabs) to the following equation:

$$(F_{experimental} - m_a F_{DNA})/(F_{complex} - F_{DNA}) = [-(1 + K_b(m_a + m_b)) + SQRT[(1 + K_b(m_a + m_b))^2 - 4m_a m_b K_b^2]]/2K_b$$

where the values of $F_{experimental}$ are the experimental fluorescence intensities (cps) along the titration profile, F_{DNA} values (cps per molar) were determined from the fluorescence intensity of the 2-aminopurine labeled oligomers alone, and m_a and m_b are the total molar concentrations of oligomer and gp32, respectively, at each point along the titration curve.

Analytical ultracentrifugation

Sedimentation velocity experiments were performed using the Beckman ProteomeLab XL-I Analytical Ultracentrifuge and sedimentation data were collected using the interference optics system. All protein and nucleic acid samples were dialyzed extensively against reference buffer, consisting of 10 mM HEPES (pH 7.5) and 30 mM KOAc, prior to centrifugation. The concentrations of both proteins and nucleic acids were re-measured after dialysis to ensure accurate final values. In each experiment 400 μl of sample and 400 μl of reference buffer were loaded, respectively, into the sample and reference sectors of a 1.2 cm double-sector Epon centerpiece and sedimented in a Beckman An60Ti ultracentrifuge rotor. Unless otherwise stated, experiments were performed at 20°C and at a rotor speed of 50 000 rpm. A partial specific volume ($\bar{v}$) of 0.732 ml/gm for gp32 protein was calculated from the amino acid composition of the protein (34). The free ssDNA constructs diffused too rapidly to form a discrete sedimentation boundary that could pull away from the meniscus and binding of the ssDNA constructs did not measurably alter the sedimentation coefficients of the gp32 components. All data analysis for the sedimentation velocity experiments was performed using the SedFit program (35–37).

RESULTS

Previous work from our laboratory and others has shown that conformational changes within nucleic acids—including base stacking and unstacking, base pairing and unpairing, and backbone extension—can all lead to changes in the low energy (near UV) circular dichroism and fluorescence spectra of 2-aminopurine (2-AP) and other nucleotide residues that can be site-specifically incorporated into DNA strands as analogs of the canonical bases. These analogs, positioned either in free nucleic acid constructs or within defined protein-nucleic acid complexes, can therefore serve as conformational probes of the local nucleic acid environment, because significant components of their spectra can be monitored at $\lambda > 300$ nm, a spectral region in which regular protein and nucleic acid components are effectively transparent (29,30). In this paper, we have used this approach to map—from the DNA perspective—the details of the interactions of gp32 with the ssDNA lattice, in order to provide a structural definition of the isolated (monomer) binding mode of this protein with ssDNA and to define the nucleic acid binding polarity of this protein. To this end we designed several 2-AP-probe-containing oligonucleotide binding constructs. These ligands are listed and defined in Table 1.

ssDNA constructs used

Previous work had shown that the site size (n) for the cooperative binding of gp32 to ssDNA lattices is 7 nts, and also that ssDNA sequences containing several adjacent dT nts bind most tightly to gp32 (22,28). In order to optimize binding affinity and to determine the binding polarity of ssDNA oligomers to gp32 monomers, our three initial ssDNA constructs contained six dT nts and a 2-AP dimer probe sequence positioned, respectively, near the 5′ end of the sequence ($_8P_{2,3}$) near the middle ($_8P_{4,5}$) or near the 3′ end of the construct ($_8P_{6,7}$) (Table 1). The 2-AP probes were not placed directly at the ends of the constructs to keep the flanking bases similar in all cases and also to avoid any ambiguity that might arise from end effects. Two additional ssDNA constructs were used in which the thymine residues were replaced with adenines ($_8A_{2,3}$ and $_8A_{6,7}$, see Table 1), with the 2-AP dimer probes positioned near either the 5′- or the 3′-ends of the 8 nts constructs to demonstrate that the results obtained were not due to ssDNA composition or sequence effects (in addition, we have used collisional fluorescence quenchers to assay the local exposure to solvent of the probe bases (see below), and for this reason also have avoided placing our probes at the ends of the ssDNA binding ligands, where they would be in uniquely exposed positions and thus mask protein-induced conformational effects.)

Oligomerization states of gp32 in the absence and presence of d(T)$_8$ lattices

It had been previously shown that at low protein concentrations gp32 exists in solution primarily as monomers, although at higher concentrations additional oligomeric states have been observed (38). To ascertain that our gp32–ssDNA binding studies reflect primarily the formation of 1:1 gp32-oligonucleotide complexes, we examined the effects of short ssDNA chains on the protein concentration dependence of gp32 oligomer formation. Sedimentation velocity ultracentrifugation methods were used to determine the association states of gp32 alone and in the presence of a representative short ssDNA lattice, d(T)$_8$. The results are shown in Figure 1 and Table 2.

Only one peak was observed in our sedimentation profiles at low gp32 concentration (1.5 μM) in the absence of ssDNA oligonucleotides, confirming earlier findings that at such concentrations gp32 exists in solution primarily as protein monomers (Figure 1A) with a $S_{20,w}$ value of ∼3.0 S (the x-axes in these plots of c(s) versus $S_{20,w}$ represent the positions of the centers of the sedimentation peaks, while (within each individual c(s) versus $S_{20,w}$ plot) the relative heights of the peaks are proportional to the fraction of the total sedimenting species that each peak represents (for further details see (35–37).) Peaks at higher $S_{20,w}$ values began to appear as the concentration of gp32 was increased

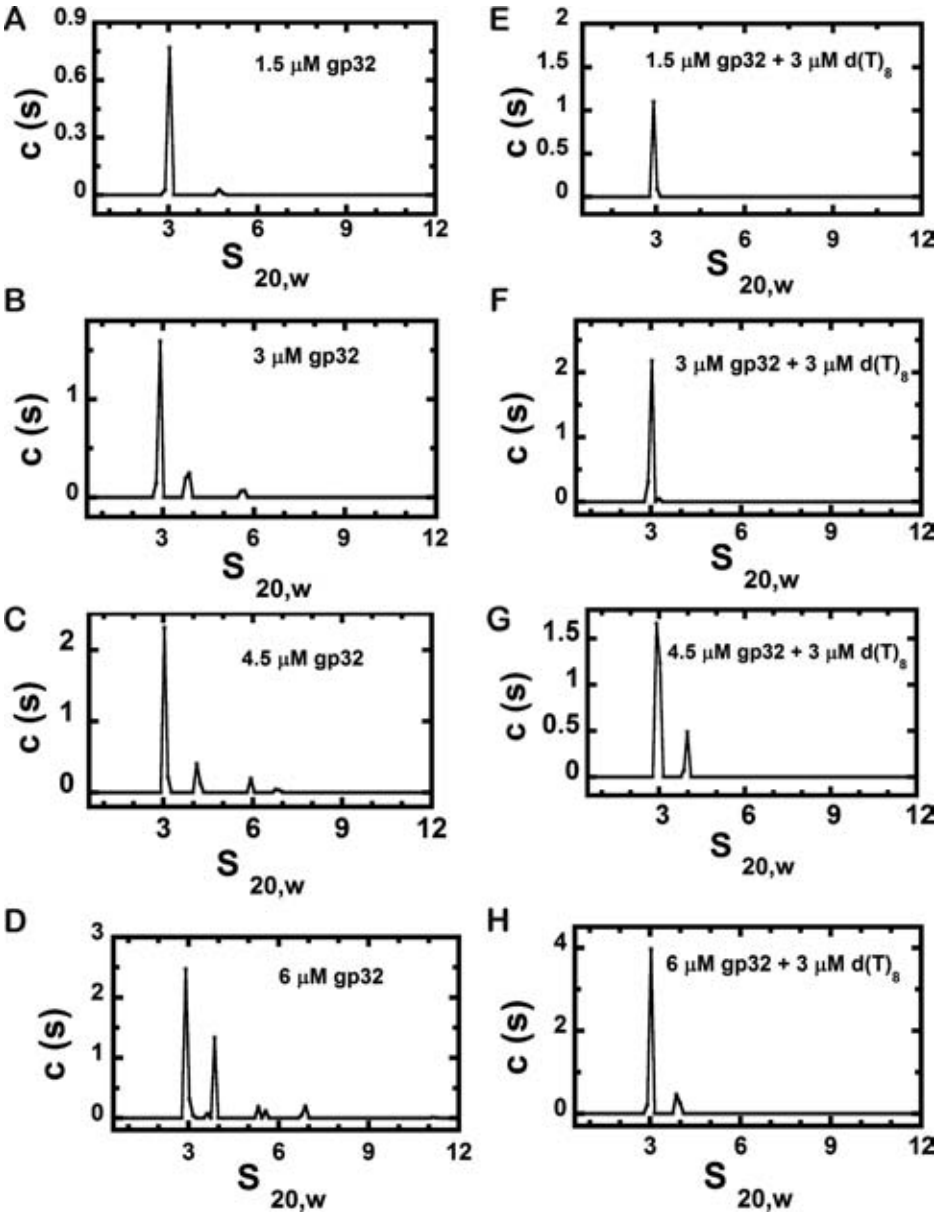

Figure 1. Oligomerization states of T4 gene 32 protein at various total protein concentrations in the absence and presence of short DNA constructs. Sedimentation velocity profiles [(c)s versus $s_{20,w}$ distribution plots] at: (**A**) 1.5 μM gp32; (**B**) 3 μM gp32; (**C**) 4.5 μM gp32; (**D**) 6 μM gp32; (**E**) 1.5 μM gp32 and 3 μM $d(T)_8$; (**F**) 3 μM gp32 and 3 μM $d(T)_8$; (**G**) 4.5 μM gp32 and 3 μM $d(T)_8$; and (**H**) 6 μM gp32 and 3 μM $d(T)_8$. The ∼3S peaks correspond to gp32 monomers (either free or bound to $d(T)_8$) and the peaks at higher $s_{20,w}$ values presumably represent dimers and higher oligomers of gp32 (see text). These experiments were performed at 20°C in buffer containing 10 mM HEPES (pH 7.5) and 30 mM potassium acetate (KOAc).

(Figure 1B–D and Table 2), confirming that higher protein concentrations led to the formation of gp32 oligomers (first dimers and then higher order species). Figure 1E–H (and Table 2) show that the addition of $d(T)_8$ suppressed gp32 oligomer formation at the same total protein concentrations used in Figure 1A–D. Thus the addition of 3 μM ssDNA to the 1.5 or 3 μM gp32 concentrations resulted in the disappearance of the (presumably gp32 dimer) peak seen at $S_{20,w}$ = 4–5 S in Figure 1A and B when gp32 alone was present. This shows that at a 1:1 molar ratio of short ssDNA lattices to gp32 at these component concentrations all the protein exists as monomers, presumably largely bound to $(dT)_8$ oligomers. We note that the 1:1 binding of a $d(T)_8$ oligomer to gp32, which increases the molecular mass of the complex by about 7% relative to that of the free gp32 monomer itself, does not result in a detectable change in the observed sedimentation coefficient. This could reflect a small increase in the asymmetry of the complex on ssDNA oligomer binding, which might then roughly offset the small increase in $S_{20,w}$ expected from the increased molecular mass of the complex. The addition of higher concentrations of gp32 (4.5 and 6 μM) to 3 μM solutions of $d(T)_8$ also resulted in a decrease in the number and size of the sedimentation peaks corresponding to protein oligomers, suggesting that the addition of short oligonucleotides to gp32 solutions disrupts small gp32 oligomers and that gp32 monomers bind in 1:1 com-

Table 2. Oligomerization of T4 gene 32 protein in the presence and absence of short DNA constructs[a]

gp32	$d(T)_8$	$s_{20,w}$ (S)	c(s)	% of each component
1.5 μM	0 μM	3.0	0.77	100%
3 μM	0 μM	2.9	1.6	86%
		3.9	0.25	14%
4.5 μM	0 μM	3.0	2.3	79%
		4.1	0.4	14%
		5.9	0.2	7%
6 μM	0 μM	2.9	2.5	60%
		3.9	1.3	30%
		5.3	0.2	5%
		6.9	0.2	5%
1.5 μM	3 μM	2.9	1.1	100%
3 μM	3 μM	2.9	2.2	100%
4.5 μM	3 μM	2.9	1.7	77%
		4.0	0.5	23%
6 μM	3 μM	3.0	3.9	89%
		3.9	0.5	11%

[a]The first two columns correspond to the input gp32 and $d(T)_8$ concentrations in each sedimentation experiment shown in Figure 1. The $s_{20,w}$ values listed in the third column represent the $s_{20,w}$ corrected sedimentation coefficients (in Svedbergs) obtained from the c(s) versus $s_{20,w}$ distribution plots for each experiment. The c(s) values listed are the measured peak heights corresponding to each sedimentation peak listed and the% values correspond to the percentage of the total protein or protein–ssDNA components in the experiment that each peak height represents. The peaks with $s_{20,w}$ values at ∼3.0S represent monomer gp32 or 1:1 gp32-$d(T)_8$ complexes. Additional peaks at higher $s_{20,w}$ values were observed as the concentration of gp32 was increased. The addition of $d(T)_8$ at each gp32 concentration resulted in a decrease in the size and number of oligomer peaks, suggesting that gp32–ssDNA complex formation competes with and disrupts gp32 protein oligomer formation (see text).

plexes with the 8-mer ssDNA. These findings are summarized quantitatively in Table 2.

Circular dichroism spectra of ssDNA oligomers containing site-specifically positioned 2-AP dimer probes define the interactions and binding polarity of ssDNA to gp32 monomers

Although the core (ssDNA-binding) domain of gp32 was co-crystallized with stoichiometric amounts of $d(T)_6$, the electron density contributed by this ssDNA lattice was not sufficiently defined to permit resolution of the structural details or the polarity of the bound oligomer (12). In principle, solution methods that can detect asymmetries in the interaction of a DNA-binding protein with the individual bases of the DNA binding target should be able to determine the polarity and at least some structural details of the binding interaction. We have looked for such asymmetries by site-specifically positioning 2-AP dimer probes near both ends and the middle of 8-mer ssDNA constructs (Table 1) and applying our base analog spectroscopic procedures (29,30) to map the interactions of gp32 with ssDNA from the perspective of the various nucleotide probe positions.

All three 8-mer ssDNA constructs (Figure 2) showed typical CD spectra (black traces) for 2-AP dimer-probe-labeled ssDNA (29,30) in the absence of gp32. The addition of increasing concentrations of gp32 to these labeled oligonucleotides resulted in a decrease in the intensity of 325 nm peak for all three probe positions, indicating that the entire ssDNA lattice is interacting with the gp32 binding surface. Figure 2A–C show that gp32 binding perturbs the CD spectra of the 2-AP dimer probes in all three positions in a qualitatively similar fashion. Furthermore the spectral changes observed are consistent with the unstacking of the 2-AP dimer probes (29,30), as might be expected as a consequence of the known ssDNA backbone extension induced by gp32 binding (26,27).

However, the 'magnitudes' of the changes in the CD spectra of the 2-AP dimer probes observed on gp32 binding depended strongly on the positions of the probes along the ssDNA construct backbones. The fractional amplitude of the intensity of the 325 nm spectral peak of the 2-AP dimer probe near the 5′-end (the $_8P_{2,3}$ construct, Figure 2A) decreased the least [by ∼10% at equimolar (6 μM) concentrations of gp32 and ssDNA oligomer], while that for the ssDNA oligomer with the probe near the 3′-end ($_8P_{6,7}$, Figure 2C) decreased the most (∼42% at equimolar ssDNA and gp32). The intensity of the 325 nm peak for the ssDNA oligomer with the dimer probe positioned in the middle of the lattice ($_8P_{4,5}$, Figure 2B) decreased by an intermediate amount (∼22% at equimolar ssDNA and gp32). The relative intensity change for each probe position as a function of added gp32 concentration is plotted in Figure 2D (control experiments were performed with unlabeled 8-mer ssDNA oligomers containing dA residues substituted for the 2-AP analogs [the sequences of the control oligomers were d(T)8, 5′d(T(A)2(T)5)3′ and 5′d((T)5(A)2T)3′], and showed that the CD spectra for all three were (within error) the same at $\lambda > 310$ nm, showing that any sequence-specific interactions between gp32 monomers and the ssDNA oligomers produced no spectral contributions in these longer wavelength regions).

Figure 2D shows that the differences in CD spectral intensity are much larger for 2-AP dimer probes located near the 3′-end of the test oligomers than for those located near the 5′-end, which is, of course, consistent with polar binding of the ssDNA oligomers to the gp32 monomer in terms of ssDNA backbone direction. Intensity changes at the central probes were intermediate. Structural molecular models for this polar binding—in both the isolated and the cooperative binding mode—that fit our observations and provide a mechanistic basis for the various functions of gp32 in regulating the various interactions of the T4 DNA replication system are presented in the 'Discussion' sections of this and the companion paper (25).

Fluorescence changes of the 2-AP dimer probes upon gp32 binding also reflect preferential interactions of the protein with the 3′-end of the ssDNA oligomers

The fluorescence quantum yield of 2-aminopurine monomers in solution is 0.68, and the incorporation of 2-AP residues into ssDNA results in significant quenching, reducing this parameter to ∼0.02 (this value depends, in part, on the identity of the flanking bases) (39,40). It has been previously shown that the peak fluorescence intensity

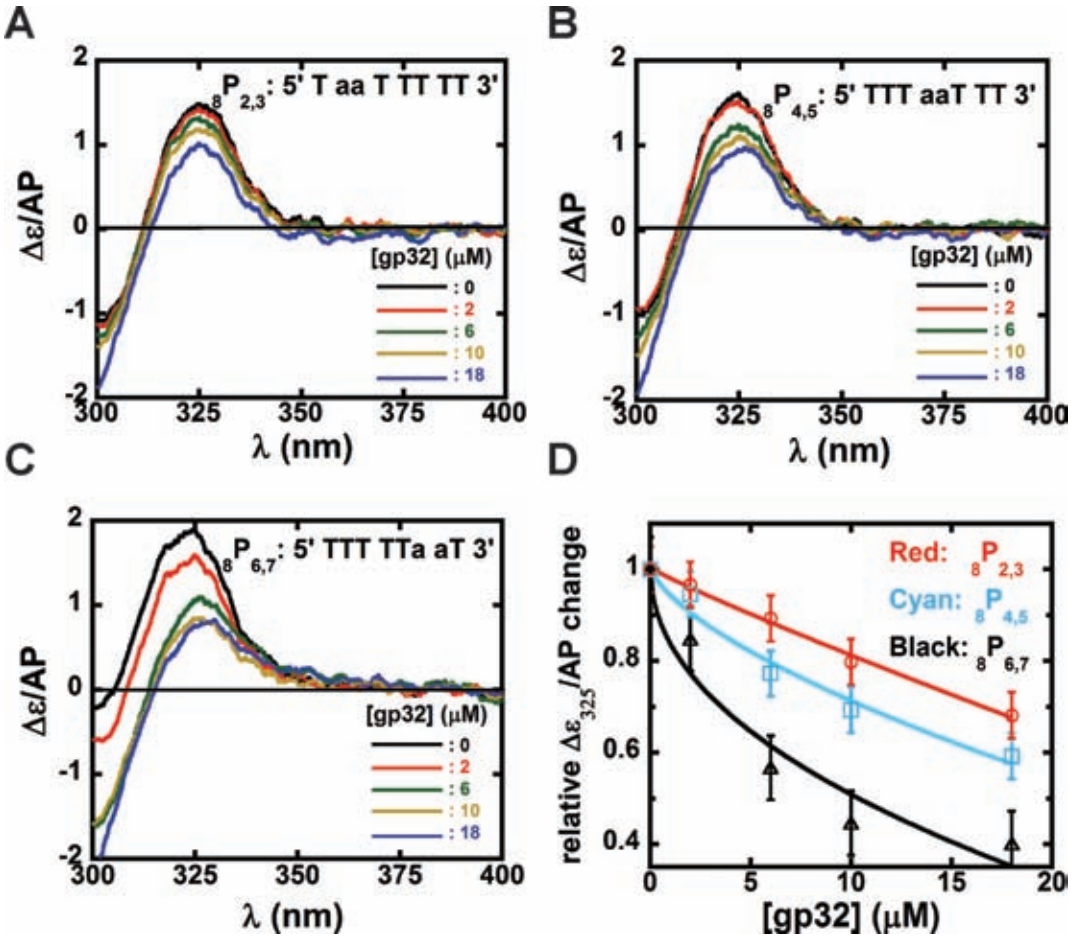

Figure 2. Circular dichroism changes observed for dT-containing ssDNA oligomers with 2-AP dimer probes at different positions. Panels **A**–**C** show changes in the CD spectra of the 8-mer ssDNA constructs following the addition of various concentrations of gene 32 protein. (A) $_8P_{2,3}$ construct; (B) $_8P_{4,5}$ construct; and (C) $_8P_{6,7}$ construct. In each panel the color-coding used for the CD spectra is: black (6 μM free DNA construct only); red (6 μM DNA and 2 μM gp32); green (6 μM DNA and 6 μM gp32); yellow (6 μM DNA and 10 μM gp32); and blue (6 μM DNA and 18 μM gp32). (**D**) Relative Δϵ/AP change at 325 nm for each ssDNA construct with increasing concentrations of gp32. $_8P_{2,3}$ construct (red, open circles); $_8P_{4,5}$ (cyan, open rectangles); and $_8P_{6,7}$ (black, open triangles). For each construct the CD at 325 nm was normalized to the protein-free values and plotted as a function of gp32 concentration. Buffer and temperature conditions same as in Figure 1.

of 2-AP probe pairs is particularly strongly self-quenched in the stacked conformation (39,40), and that the fluorescence of these probe pairs increases significantly on probe unstacking and exposure to the solvent environment. Based on the same reasoning discussed in the context of the CD spectral changes observed with these dimer probes with gp32 binding, where unstacking was reflected in decreases in intra-dimer-probe exciton coupling (Figure 2), we expect that unstacking of the probe bases due to backbone extension should result in major 'increases' in fluorescence intensity at 370 nm and the differences in the amplitudes of the increases observed at the three probe positions on gp32 addition should reflect differences in the local interactions of the three probe pairs with the solvent environment and the amino acid residues of the binding surfaces of the gp32 monomers.

Figure 3A–C show the fluorescence spectra of the three 8-mer constructs at several concentrations of added gp32, confirming that increases in the magnitudes of the fluorescence spectra of the three 8-mer ssDNA constructs are indeed observed with increasing bound gp32. As seen in studies of other protein–DNA interaction systems using 2-AP probes, the *shapes* of the fluorescence spectra of the oligomer probes are unchanged by gp32 binding, and thus the effects of increased gp32 can be monitored quantitatively by tracking the fluorescence intensity at 370 nm and plotting as a function of added gp32 concentration. Normalized plots of these data are presented in Figure 3D for all three 8-mers, and show that all three binding isotherms follow the shape expected for 1:1 complex formation, although the fractional amplitudes of the fluorescence changes differ significantly from one construct to another. All three showed an increase in fluorescence intensity, suggesting (in keeping with the CD spectral results shown in Figure 2) that gp32 binding caused some extension of the ssDNA backbone at all the probe positions, although we note that the amplitude increase for the $_8P_{6,7}$ was about one half of the amplitude increase for the other two constructs. This observation is consistent with the results of the acrylamide

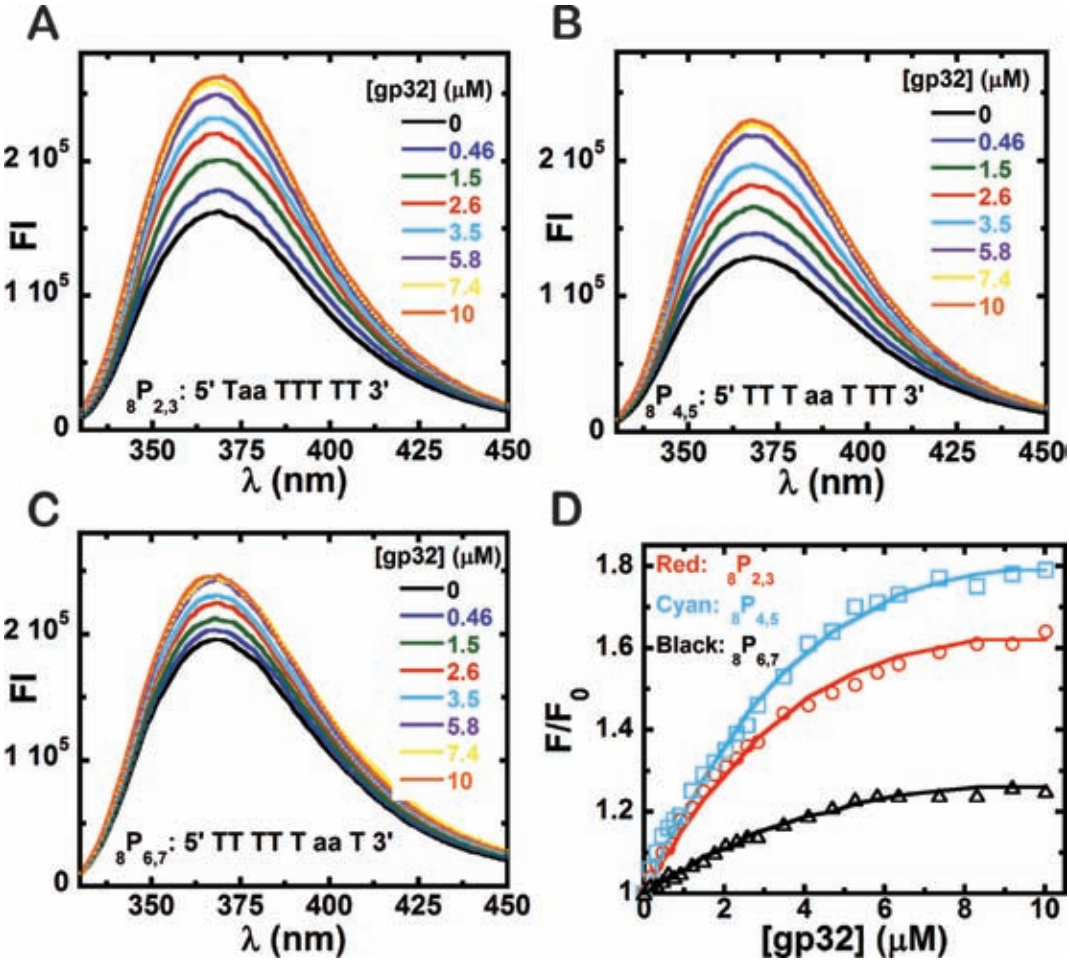

Figure 3. Fluorescence intensity changes observed for dT-containing ssDNA oligomers with 2-AP dimer probes at different positions. Panels **A**–**C** show changes in the raw fluorescence emission intensity of the 8-mer ssDNA constructs following the addition of various concentrations of gene 32 protein. Titration isotherms for (A) the $_8P_{2,3}$ construct; (B) the $_8P_{4,5}$ construct; and (C) the $_8P_{6,7}$ construct. In each panel the color-coding used for the fluorescence emission spectra is same as that used for the gp32 concentration shown in the box in each panel. (**D**) Normalized fluorescence intensity change at 370 nm for each ssDNA construct with increasing concentrations of gp32. Panel D plots the fluorescence intensity changes at 370 nm for the three 8-mer 2-AP dimer-probe-labeled ssDNA constructs (3 μM) as a function of input gp32 concentration: $_8P_{2,3}$ construct (red, open circles); $_8P_{4,5}$ (cyan, open rectangles); and $_8P_{6,7}$ (black, open triangles). The spectral data were normalized as in Figure 2D, but here using the intensity of the 370 nm fluorescence peak. Buffer and temperature conditions as in Figures 1 and 2.

quenching experiments as a function of 2-AP dimer probe backbone position (see below).

Binding affinities of gp32 monomers for the 8-mer ssDNA oligomers

The relative intensities of the 325 nm peaks of the CD spectra for each probe-containing oligomer, plotted in Figure 2D as a function of added gp32 concentration, showed that the observed changes for all the constructs decreased approximately linearly with gp32 concentration in the initial part of the titration (although with some indication of approaching binding plateaus) over the concentration range tested. Although the magnitude of the overall peak intensity decrease differed significantly for the variously positioned spectral probes, in keeping with a clearly defined binding polarity, the consistent downward trend of the plots of Figure 2D also suggests that the CD spectral change at all positions did not reach saturation over this range of gp32 concentrations. This is in accord with earlier studies of gp32 binding to short ssDNA oligomers, which showed the dissociation constants (K_d) for these interactions to be of the order of 10^{-5} M, comparable to the concentrations of the gp32 and ssDNA components used in these experiments. Thus, in keeping with the observations of Figure 2D, our test oligomers were also not fully saturated with gp32 at 1:1 molar ratios of the components in these fluorescence titrations.

The increases in the fluorescence intensity changes for the 2-AP dimer probes in ssDNA (29,30) reflect the unstacking of the 2-AP pairs as a consequence of the binding of the gp32 to the 8-mer constructs, and can be used to obtain accurate K_d values for the binding of gp32 to our various 8-mer ssDNA probe constructs. Such titrations, conducted with 3 μM concentrations of ssDNA oligomer molecules in each case and monitored at 370 nm (the peak intensity of the probe fluorescence for each of our 8-mer constructs) are shown in Figure 3A–C for the $_8P_{2,3}$, $_8P_{4,5}$ and $_8P_{6,7}$ con-

Table 3. Binding constants and contributions of the individual components (free ssDNA and protein–ssDNA complex) to the total fluorescence intensity calculated from the titration data of Figures 3D, 5B and 5E.[a]

Oligomer	K_d (10^{-5} M)	$F_{complex}$ (10^{11} cps/M)	$F_{complex}/F_{DNA}$
$_8P_{2,3}$	0.35 ± 0.04	1.26	2.4
$_8P_{4,5}$	0.42 ± 0.04	1.18	2.8
$_8P_{6,7}$	1.03 ± 0.10	1.42	2.1
$_8A_{2,3}$	0.41 ± 0.04	1.74	1.5
$_8A_{6,7}$	0.32 ± 0.03	2.06	1.7

[a]The titrations were monitored by tracking the 2-AP fluorescence of the ssDNA oligomer at 370 nm in each experiment. The first column identifies the oligomers, the second shows the calculated dissociation constants, the third shows the raw data for the fraction of fluorimeter counts in the gp32–ssDNA oligomer complex and fourth is the ratio of the fluorescence intensity of the complex to that of the free oligomer at the point in the titration curve at which the ratio of input gp32 concentration to total $d(T)_8$ is 1:1.

structs, respectively. The K_d values (calculated as described in 'Materials and Methods' section) are summarized in Table 3.

The K_d values obtained for the three ssDNA constructs in the fluorescence titrations are of comparable magnitude, as expected from the binding results for the unlabeled oligomers, but showed a small 'increase' (weaker binding) as the dimer probe was moved from the 5′-end of the oligomer ($_8P_{2,3}$; $K_d = 0.35 \times 10^{-5}$ M) to the middle ($_8P_{4,5}$; $K_d = 0.42 \times 10^{-5}$ M) and then to the 3′-end ($_8P_{6,7}$; $K_d = 1.0 \times 10^{-5}$ M). This trend is consistent with the notion that gp32 binds less tightly to the constructs with 2-AP dimer probe at the 3′ end ($_8P_{6,7}$ construct), presumably because the direct binding of gp32 to the purine-containing probes requires that some of the binding free energy be used to unstack the 2-AP probe bases, while direct binding to a pair of dT residues at the 3′-end of the 8-mer ssDNA construct would require the consumption of less binding free energy for base unstacking.

The binding affinities for gp32 monomers of various 'homomeric' oligonucleotides ranging from 2 to 8 nts in length have been previously measured using an intrinsic protein fluorescence quenching assay (15). The values of K_d obtained were ∼0.4 x10^{-5} M for $d(T)_8$ and ∼0.6 × 10^{-5} M for $d(A)_8$. The observation that the K_d values of $_8P_{2,3}$ and $_8P_{4,5}$ constructs are very similar to those obtained for the $d(T)_8$ construct by protein fluorescence quenching is in good agreement with our suggestion that gp32 interacts most directly with ssDNA oligomers near the 3′ end. As a consequence, the substitution of thymine bases at other positions should not significantly alter the observed K_d value. However, positioning the 2-AP dimer probe near the 3′ end, where we infer that gp32 binds most tightly and directly, 'increased' K_d slightly, with the observed value shifting toward that obtained for constructs containing only adenine residues (see below). These values are close to those obtained with our 8-mer ssDNA constructs, showing that binding of the 2-AP probes in all the positions examined are likely to be very similar to those of the canonical dA residues that they replaced.

Acrylamide quenching confirms preferential 3′-end binding of short oligomers to gp32 monomers

Acrylamide monomers in solution can serve as neutral collisional quenching agents, and their quenching efficiencies in different contexts depend on the accessibility of the 2-AP dimer probes to the aqueous solvent (29,32,41). Here acrylamide quenching was used to study the solvent accessibility of probe bases at various positions of our 8-mer ssDNA constructs in both the free and the gp32-bound states. Increasing concentrations of acrylamide were added to 3 μM concentrations of DNA constructs at 0, 3 or 6 μM concentrations of gp32 monomers, respectively, and the results are presented as Stern–Volmer plots in Figure 4.

Figure 4A shows that the presence or absence of gp32 does not change the quenching efficiency of acrylamide for oligonucleotide constructs in which the 2-AP dimer probes are located near the 5′-terminus of the ssDNA oligomer (the $_8P_{2,3}$ construct). In contrast a small decrease in quenching is observed for gp32 binding for constructs with 2-AP in the middle ($_8P_{4,5}$) (Figure 4B) and a larger collisional quenching effect (but still demonstrating significantly incomplete protein 'shielding' of the probes) is shown for the 2-AP dimer pairs at the 3′-end of the construct ($_8P_{6,7}$). These results are consistent with a protein binding interaction that leaves the probe bases largely exposed, but partially shields those at the 3′-end of the construct, likely as a consequence of direct binding of gp32 residues to adjacent sugar-phosphate backbone positions. The probe bases located at the 5′-end (or close to the middle) of the oligomer constructs may be less perturbed by this collisional quenching agent because they are only weakly (and presumably not 'site-specifically') bound to the gp32 interaction surface, perhaps by weaker and less localized charge-charge interactions (see 'Discussion' section).

This trend, showing progressively less collisional shielding for the probes on the 5′-end of the 8-mer ssDNA constructs, is fully consistent with the same trend seen in Figure 2A–C, which shows a diminishing perturbation of intra-2-AP dimer exciton coupling as the probes are shifted from the 3′- to the 5′-end of the constructs. Thus these acrylamide quenching findings comprise a separate (and consistent) determination of the binding directionality of the ssDNA chains to the gp32 monomers.

Preferential binding of gp32 near the 3′ end of ssDNA oligomers is not sequence specific

The binding of gp32 monomers to short ssDNA oligomers is relatively independent of the base composition and sequence of the oligomers, except that oligomers containing multiple adjacent dT residues bind as much as three-fold more tightly. In order to ascertain that the binding polarity that we have observed in this study does not reflect some form of sequence specificity based on the presence of multiple contiguous thymine residues, 2-AP dimer probes were site-specifically placed into oligomers containing flanking adenine bases only (Table 1). To this end oligonucleotide constructs were designed that contained six adenines and 2-AP dimer probes positioned near either the 5′- or the 3′-

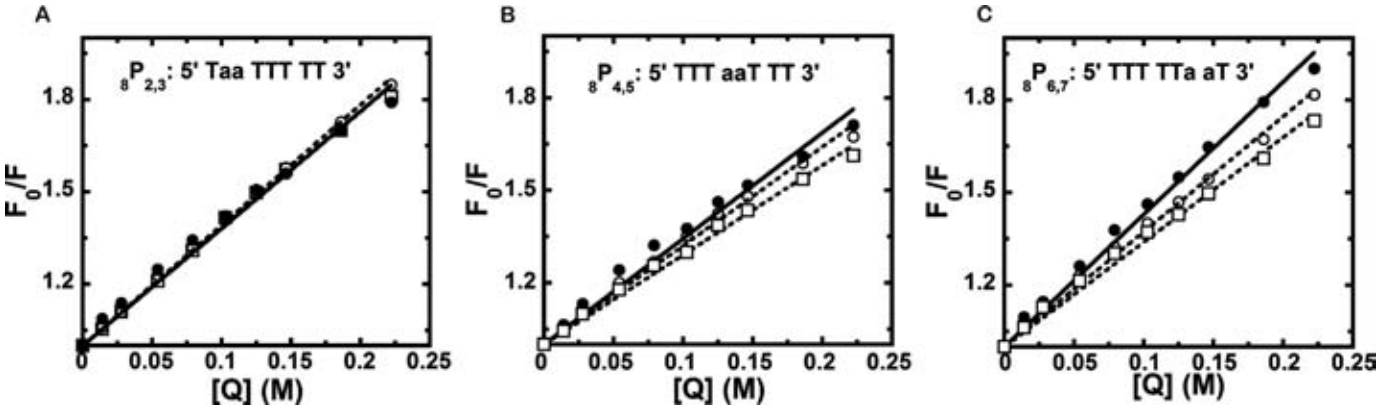

Figure 4. Stern–Volmer plots for fluorescence quenching by acrylamide of dT-containing ssDNA oligomers with 2-AP dimer probes at different positions in the absence (solid lines) and presence (dashed lines) of gp32 monomers. (**A**) $_8P_{2,3}$ construct (3 μM free DNA, filled circles; plus 3 μM gp32, open circles; plus 6 μM gp32, open squares). (**B**) $_8P_{4,5}$ construct (3 μM free DNA, filled circles; plus 3 μM gp32, open circles; plus 6 μM gp32, open squares). (**C**) $_8P_{6,7}$ construct (3 μM free DNA, filled circles; plus 3 μM gp32, open circles; plus 6 μM gp32, open squares). Buffer and temperature conditions as in Figures 1 and 2.

termini. These constructs were designated $_8A_{2,3}$ and $_8A_{6,7}$ respectively (Table 1).

The CD spectra of both constructs were measured (Figure 5A and D), and showed that the construct with 2-AP dimer probes near the 5′ region ($_8A_{2,3}$) was unaffected by gp32 binding, whereas the CD spectrum of the oligonucleotide construct with 2-AP dimer probes at the 3′ region ($_8A_{6,7}$) was perturbed in a similar way to that observed for the $_8P_{6,7}$ construct containing thymines as flanking bases (compare with Figure 2A and C). Fluorescence titrations of gp32 monomer binding to $_8A_{2,3}$ and $_8A_{6,7}$ constructs were conducted with 3 μM concentrations of oligomer molecules in each case and monitored at 370 nm and are shown in Figure 5B and E, respectively. The values obtained for K_d are summarized in Table 3. The observed K_d values for both constructs are similar, which is expected, because 2-AP is the fluorescent base analog of adenine and we expect it to stack similarly to dA. The contribution of the DNA–protein complex to the total intensity also follows the same trend and the very slight increase in binding affinity observed with the $_8A_{6,7}$ construct is reflected in both the binding constant and the fluorescence intensity amplitude change data.

Acrylamide quenching experiments were also performed with these constructs, and again the $_8A_{2,3}$ construct showed no significant change on the addition of 200 mM acrylamide, while a significant decrease in quenching was observed on gp32 binding for the $_8A_{6,7}$ construct (Figure 5C and F). This result is consistent with the CD data (Figure 5A and C) and also with the results obtained with thymine-containing sequences (compare with Figure 4A and C). This result also confirms that the binding asymmetries seen between the 5′- and the 3′-regions of the oligomer constructs reflect gp32 interaction differences that are based on backbone polarity, and not on base sequence effects.

DISCUSSION

As pointed out in the 'Introduction' section, the DNA replication system of bacteriophage T4 functions with relatively few protein components, and T4 is probably the simplest creature that manifests the organizational principles characteristic of the replication systems of most higher organisms. This makes it an excellent model system to study many of the interactions that regulate the function of the genome. The single-stranded binding (ssb) proteins of most well studied DNA replication systems are central to the functioning and integration of these important and much-studied macromolecular machines, and relatively minor changes in the properties or concentrations of these proteins are often enough to derange the orderly processes of genome expression. We note, however, that the binding cooperativity properties of the ssb proteins differ between T4, *E. coli* (9) and higher organisms (42), suggesting that this parameter may play somewhat different physiological roles in these various systems.

Gp32, at least, appears to be relatively simple. It has no enzymatic activity and can be characterized by single binding (K) and cooperativity (ω) parameters, but it is responsible for the regulation of many important physiological functions of the T4 replication system, primarily involving the binding, protecting and packaging of the ssDNA sequences that serve as transient functional intermediates (usually as polymerase templates) in virtually all the processes of genome metabolism and expression. To this end gp32 must fully coat the transient single-stranded intermediates within the replication 'trombone' complex (43), and do this in a way that facilitates the activities of the other components of replication system, including the helicases, polymerases and clamp loaders whose smooth and integrated interactions are required for organized cellular activity.

The binding of gp32 and related ssb proteins has been much studied, and the biological functions of these proteins can be largely understood in terms of the thermodynamics and kinetics of their binding to the single-stranded DNA intermediates of the replication process as these intermediates are exposed by the replication helicase, utilized (as templates) by the replication polymerases, and then restored to the duplex form by displacement of the gp32 by the polymerase and other proteins that drive the orderly manipula-

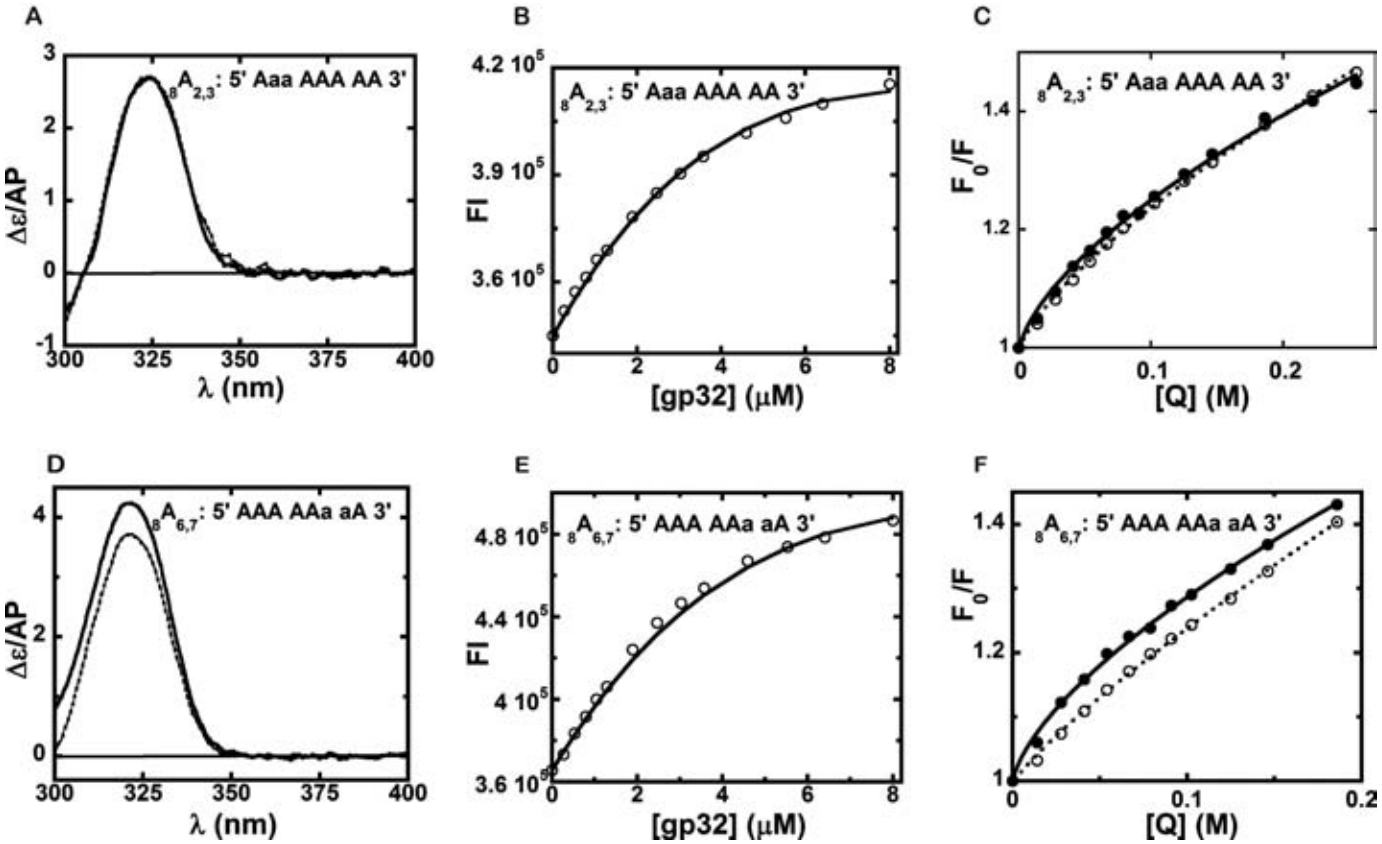

Figure 5. Circular dichroism spectra, fluorescence intensity titrations and acrylamide quenching for DNA constructs with 2-AP dimer probes site-specifically positioned in 8-mer ssDNA constructs containing only adenine residues. (**A**) CD spectra for the 3 μM $_8A_{2,3}$ construct in the absence and presence of gp32 monomers (free DNA, solid line; plus 3 μM gp32, dotted line). (**B**) Fluorescence intensity changes observed for 3 μM $_8A_{2,3}$ construct at 370 nm plotted against the input gp32 concentration. (**C**) Acrylamide quenching of the 3 μM $_8A_{2,3}$ construct in the absence and presence of 3μM gp32 monomers (free DNA, solid line, filled circles; plus gp32, dotted line, open circle). (**D**) CD spectral changes for the 3 μM $_8A_{6,7}$ construct in the absence and presence of gp32 monomers (free DNA, solid line; plus 3 μM gp32, dotted line) (**E**) Fluorescence intensity changes observed for 3 μM $_8A_{6,7}$ construct at 370 nm plotted against the input gp32 concentration. (**F**) Acrylamide quenching of 3 μM $_8A_{6,7}$ construct in the absence and presence of 3 μM gp32 monomers (free DNA, solid line, filled circles; plus gp32, dotted line, open circles). Buffer and temperature conditions as in Figures 1 and 2.

tion of the genome. An equilibrium theory to describe the overlap and cooperative binding of ssb proteins to long ssDNA lattices had been previously developed and tested (24) and the binding parameters (site size, binding constant and cooperativity parameter) for several ssb protein systems, including gp32 (14,15,18,19,22), have been carefully determined. In addition some kinetic parameters for the binding and dissociation of gp32 to ssDNA lattices have also been estimated using both bulk solution (15,16) and single molecule DNA stretching (18–20) methods. However, these measurements all depend on molecular signals (intrinsic protein fluorescence changes, kinetics of the reversal of DNA stretching, etc.) that are not subject to direct interpretation in terms of details of protein or DNA structure.

In this study, we have examined changes induced by gp32 binding in the fluorescence and circular dichroism spectra of DNA analog bases that have been site-specifically placed into defined short ssDNA constructs, and show that analysis of these changes permits molecular interpretations of these binding parameters and interactions (from the perspective of the ssDNA binding targets) at single base resolution. Based on these observations, as well as on binding models developed previously in earlier studies (15,21), a molecular model for gp32 binding to short ssDNA lattices is here proposed that can serve also as a basis for understanding the binding, unbinding and interactions of cooperatively bound gp32 clusters as described in the companion paper (25).

Binding polarity and detailed protein–ssDNA interactions

The results of this paper demonstrate that the binding of short ssDNA lattices to gp32 monomers is asymmetric with respect to the protein surface, and exhibits polarity in terms of the orientation of the sugar-phosphate backbone of the DNA. This is clearly demonstrated by the differences between the CD and fluorescence spectra of dT-containing ssDNA 8-mer lattices containing 2-AP dimer probes located near the 5′- or the 3′-ends of the construct, with intermediate behavior seen for dimer probes located near the centers of the 8-mer lattice (Figures 2 and 3). The CD spectra show directly that the exciton interactions between the 2-AP bases of the dimer probe are significantly more decoupled for probe pairs positioned near the 3′-end of the lattice than for probe pairs near the 5′-end, suggesting that the 2-AP

bases located near the 3′-end of the 8-mer ssDNA lattices are significantly more unstacked.

This unstacking interpretation can be extended by considering the fluorescence enhancement findings shown in Figure 3 in conjunction with the acrylamide quenching experiments of Figures 4 and 5. These acrylamide measurements, in particular, demonstrated that the interactions with gp32 of probes near the 3′-end of the 8-mer show a significant 'decrease' in exposure to these collisional quenching agents, while probes near the center of the 8-mer ssDNA lattice show an intermediate decrease and those near the 5′-end show essentially no change in access to the quencher. Equivalent changes in CD spectra and acrylamide access are shown for lattices containing dA-residues at all the non-probe lattice positions, indicating that these asymmetric effects of binding depend primarily on the 'positions' of the 2-AP dimer probes within the ssDNA lattices of the 8-mers, and that the base composition and sequence surround of the dimer probes do not effect the binding polarity observed as a function of probe position.

Inspection of the crystal structure of the core DNA-binding domain of gp32 (Figure 6A) suggests that this decrease in access to collisional quenchers near the 3′-end of the 8-mer ssDNA constructs might reflect partial intercalation into the ssDNA chain at these positions of tyrosine side-chains within the DNA binding cleft (see (12)), which could be an additional determinant of the proposed backbone twisting and chain extension resulting from the tight binding of the gp32 to the sugar-phosphate backbones of the ssDNA chain near the 3′-end of the test oligomers.

It is important to appreciate that our results do *not* provide direct information on the directionality of oligomer binding relative to the structure of the gp32 monomer itself, but here the crystal structure of the DNA binding (or 'core') domain of gp32 (12) provides some clues. Figure 6B shows the structure of the core domain, with the first four residues of a bound $(dT)_6$ chain modeled in. As mentioned in the 'Introduction' section, while the core domain was crystallized together with a 6-mer oligo(dT) lattice, the quality of the non-protein electron-density was not sufficient to reveal either the backbone polarity or the structural details of the bound ssDNA. The electron-density was best defined at the left-hand end of the chain shown in Figure 6B, with the rest of the ssDNA electron density fading off to the right within the putative ssDNA binding cleft. Shamoo *et al*. (12) labeled the left end of the oligomer that they modeled in as the 5′-end of the chain, and the right end as the 3′. However, our results suggest the reverse, namely that the best defined and extended section of the chain shown on the left in Figure 6B is likely the 3′-end of the (dT_6) sequence, and the more poorly defined section of the sequence that faded off toward the right side of the figure probably corresponds to the 5′-end.

Binding constants for gp32 monomers to 8-mer ssDNA lattices

Our sedimentation velocity measurements (Figure 1) confirmed that the binding interactions we have studied here can be treated as 1:1 interactions between a single native gp32 monomer and the various 8-mer ssDNA constructs. The binding constant measurements (Figure 3 and Table 3) support this picture and provide further molecular details. In accord with earlier measurements (14,16,18,19), the dissociation constant (K_d) for all of our binding interactions between the 8-mer ssDNA constructs and the native gp32 monomer fall in the vicinity of 10^{-5} M. Given that the concentrations of the components used in the measurements are also of this same order of magnitude, binding is clearly incomplete (Figure 3), with the components of the complex at equimolar concentrations of gp32 and ssDNA oligomer ranging from 30 to 50% bound and 70 to 50% free. However (see Table 3), the 'differences' between the K_d values for the different constructs do lie outside the limits of error and therefore tell us something significant about how the energetics of the binding interaction differ for the 8-mer ssDNA constructs with the probes in different positions.

We have argued above (primarily on the basis of CD and fluorescence data) that the dimer probes within the bound ssDNA constructs are more unstacked near the 3′-ends than near the 5′-ends of our test ssDNA oligomers. This interpretation is supported by our equilibrium binding titration curves, which show that K_d is larger (binding is weaker) when the 2-AP bases within the probes are unstacked by the binding interaction near the 3′-end, while when dT residues are in this position unstacking requires less binding free energy and thus K_d values are smaller. For oligomers containing only dA (and 2-AP) residues, no significant differences in K_d were observed as a function of probe position (Table 2), as expected if the stacking free energies of adjacent 2-AP bases and adjacent adenine bases within the ssDNA constructs are about the same.

These results, and the spectroscopic findings summarized in the previous section, are all consistent with a structural proposal that the gp32 monomer interacts most tightly and specifically with the residues near the 3′-end of our short ssDNA constructs—probably by binding primarily to the sugar-phosphate bonds at this end of the structure and untwisting the ssDNA—thus forcing the bases apart and extending the oligomer. We suggest that the accompanying modest 'decrease' in the exposure of the bases to collisional quenchers (and solvent) may reflect interactions of the separated bases with amino acid residues in the binding surface of gp32, most plausibly the several tyrosine side-chains that are present in the binding cleft of the gp32 core domain and may intercalate (and partially stack?) with the separated 2-AP bases of the dimer probe. We suggest that the interactions between the oligomer residues at the 5′-end of the chain and the gp32 monomer surface are weaker and primarily electrostatic (see below), although—probably because of the placement of the basic residues on the protein binding surface—these interactions also serve to extend the chain somewhat (Figures 2 and 5), and concomitantly to increase the fluorescence signal (also attributed to 2-AP dimer unstacking) that we have used to determine K_d values (Figures 3 and 5).

The role of the C-terminal arm of the native gp32 protein

We remind the reader that the crystal structure of the core domain of gp32 shown in Figure 6A and B is missing both the N- and the C-terminal domains of the native protein,

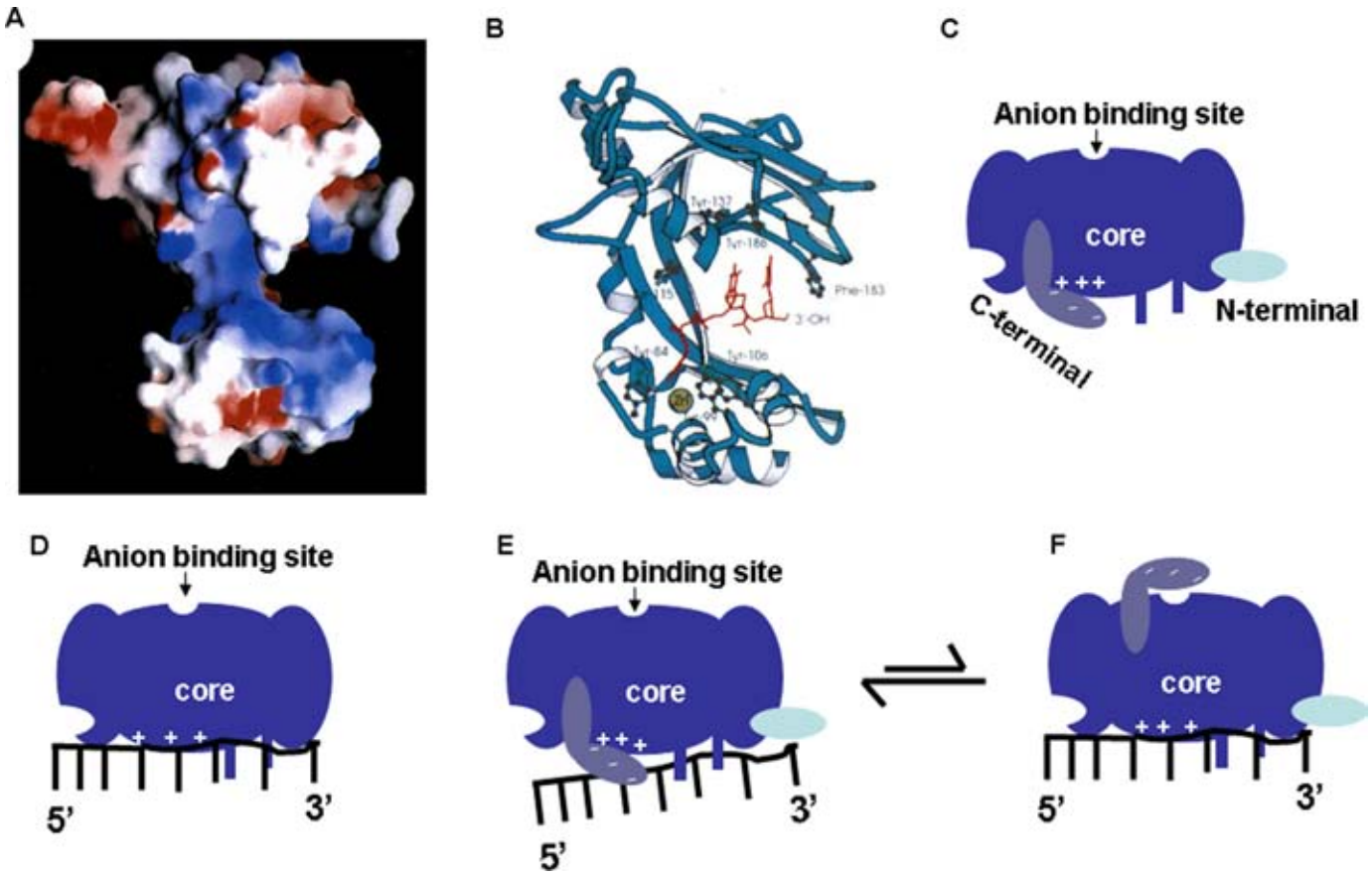

Figure 6. A model for the binding of single gp32 molecules to short ssDNA lattices. (**A**) Representation of the structure and electrostatic surface potential of the core domain of gp32; blue regions are basic and red regions are acidic (12). (**B**) The core gp32 domain with a bound ssDNA $d(T)_4$ oligonucleotide fitted to the difference electron density (12). (**C**) Model of an isolated gp32 molecule showing the C-terminal arm tightly bound to the electropositive cleft of the core domain in the absence of ssDNA. (**D**) Model of the core gp32 domain bound to an 8-mer ssDNA lattice. The absence of the C-terminal flap allows the oligonucleotide to 'shuffle' along the protein lattice. (**E**) Model of the binding of a gp32 monomer to an 8-mer oligonucleotide. The positively charged binding cleft of the core domain is occluded by the C-terminal arm, thereby hindering the access of the oligonucleotide and resulting in more base unstacking at the 3′ end and less at the 5′ end of the 8-mer ssDNA lattice. This is represented by the decreasing gradient of chain extension from the 3′ to the 5′-end of the ssDNA oligomer. We suggest that this binding mode is likely to be in dynamic equilibrium with a gp32 monomer conformation (**F**) in which the C-terminal arm is flipped out of the positive binding cleft and binds to the previously proposed anion binding site (14,15) on the 'top' of the gp32 monomer, displacing bound monovalent anions there and permitting full oligonucleotide access to the gp32 binding cleft. Panels (A) and (B) of this figure have been reproduced, with permission, from (12).

and that these domains are respectively critical for interactions of the gp32 molecule with the other proteins of the replication complex (the 48 residue C-terminal domain) and for binding cooperativity (the 21 residue N-terminal domain). Thus these 'arms' clearly play a role in cooperativity and regulation, as further discussed in the companion paper (25). Both arms are present in the native gp32 monomers whose binding we study here (shown in Figure 6C, E and F), and the C-terminal domain, in particular, plays an important role in the binding of the gp32 monomer.

Earlier titration experiments of gp32 monomers with short ssDNA oligomers, using primarily changes in intrinsic protein fluorescence signals (14,15,22), provided important thermodynamic data for gp32 monomer binding to short ssDNA lattices. The results of the present study now permit molecular interpretations of some of those binding parameters. These earlier measurements had shown that while binding studies of gp32 to long ssDNA lattices demonstrated that the occlusion site size for a cooperatively bound gp32 monomer was 7 nts, the measured binding affinity of gp32 monomers for short lattices was constant for ssDNA oligomers ranging in length from 2 to 8 nts, and that the binding parameters for the native gp32 monomers showed essentially no salt concentration or nucleotide sequence or composition dependence. In contrast, binding to the gp32 core domain from which the N- and C- terminal domains had been removed (this truncated domain is shown in Figure 6A, B and D was designated gp32*III in the earlier literature) showed a slightly smaller binding site size, and the binding of this moiety to ssDNA oligomers did show both lattice length and some salt concentration dependence.

These results, together with our present demonstration of binding polarity and asymmetry, showed that the most energetically significant binding interaction occurs with 2–3 nts located at or near the 3′-end of the test oligomers, and can be interpreted in terms of the schematic gp32 models shown in Figure 6D (for binding to the core domain) and Figure 6E and F (for binding to the native gp32 monomer).

These cartoons emphasize, for both the gp32 core domain and the full-length native gp32 monomer, that the major contribution to the binding interaction involves the first 2–3 nts at the 3′-end of the test oligomer, where localized interactions involve tight binding to (and presumably distortion of) the sugar-phosphate backbone as described above. The 8-mer ssDNA oligomers also have access to, and show some binding affinity for, the positively charged binding cleft of the truncated (C- and N-terminal domains removed) core domain (12), thus accounting for the fact that the binding to this domain is higher at lower salt concentrations (electrostatics) and increases also with oligomer length (presumably because of the possibility for statistical 'shuffling' of the tight 2–3 nts binding site on the protein into various positions on the ssDNA lattice), thus increasing the apparent binding constant of the test ssDNA oligomer as a function of ssDNA lattice length (44–46).

In contrast, for the native gp32 monomer the positively charged binding cleft is occluded by the binding of the negatively charged C-terminal arm (Figure 6E), thus exposing only the 2 nts tight binding site of the gp32 monomer for interaction with the 8-mer ssDNA oligomer. This results in making unavailable both the electrostatic binding of 5′ portion of the ssDNA lattice into the positively charged binding cleft and the expected dependence of the measured K_d on the length of the lattice, the latter by removing the possibility of 'statistically shuffling' the tight-binding site into the other lattice positions. In cooperative gp32 binding (25) the C-terminal arm also swings to an alternative anion binding site located on the 'top' of the gp32 monomer (Figure 6F), presumably displacing the tightly-bound anions from this site (14,15) and thus exposing the DNA binding cleft of the protein for electrostatic binding with the rest of the ssDNA of the lattice. It is likely that the binding of the C-terminal arm in the binding cleft and to the 'top' position on the gp32 monomer is subject to a conformational equilibrium (Figure 6E and F), with the binding of the rest of the lattice in the binding cleft not significantly changing the overall free energy change associated with gp32 monomer binding because the electrostatic binding free energy lost by the displacement of the C-terminal arm of the protein from the core domain binding cleft is largely compensated by the electrostatic binding free energy gained by the binding of the 5′-terminus of the oligomer lattice. Somewhat similar conclusions on this point, based on earlier data, were included in the binding models for gp32 as a function of salt concentration earlier put forward by Rouzina *et al*. (21), building on the still earlier models of Kowalczykowski *et al*. (15). As also pointed out by Pant *et al*. (19), the dynamics of this displacement of the C-terminal arm of the gp32 may well be a function of salt concentration, and this hypothesis appears to be consistent with the results of kinetic studies of the gp32–ssDNA interaction that are currently in progress (W. Lee, J. Gillies, C. Phelps, B. Israels and D. Jose, unpublished experiments).

ACKNOWLEDGEMENT

We are grateful to our colleagues in both the Andrew Marcus and the von Hippel laboratories for many helpful discussions of this work, and to Miya Mary Michael for help in preparing and purifying the T4 gene 32 protein used in these studies.

FUNDING

NIH [GM-15792 to P.H.v.H]. Funding for open access charge: NIH [GM-15792].
Conflict of interest statement. None declared.

REFERENCES

1. Johnson,A. and O'Donnell,M. (2005) Cellular DNA replicases: components and dynamics at the replication fork. *Annu. Rev. Biochem.*, **74**, 283–315.
2. Mueser,T.C., Hinerman,J.M., Devos,J.M., Boyer,R.A. and Williams,K.J. (2010) Structural analysis of bacteriophage T4 DNA replication: a review in the Virology Journal series on bacteriophage T4 and its relatives. *Virol. J.*, **7**, 359–375.
3. Nossal,N.G. (1994) *Molecular Biology of Bacteriphage T4*. American Society for Microbiology, Washington, D.C.
4. Alberts,B.M. (1987) Prokaryotic DNA replication mechanisms. *Philos. trans. R. Soc. Lond. B. Biol. Sci.*, **317**, 395–420.
5. Jose,D., Weitzel,S.E., Jing,D. and von Hippel,P.H. (2012) Assembly and subunit stoichiometry of the functional helicase-primase (primosome) complex of bacteriophage T4. *Proc. Natl. Acad. Sci. U.S.A.*, **109**, 13596–13601.
6. Alberts,B.M. and Frey,L. (1970) T4 bacteriophage gene 32: a structural protein in the replication and recombination of DNA. *Nature*, **227**, 1313–1318.
7. Villemain,J.L., Ma,Y., Giedroc,D.P. and Morrical,S.W. (2000) Mutations in the N-terminal cooperativity domain of gene 32 protein alter properties of the T4 DNA replication and recombination systems. *J. Biol. Chem.*, **275**, 31496–31504.
8. von Hippel,P.H., Kowalczykowski,S.C., Lonberg,N., Newport,J.W., Paul,L.S., Stormo,G.D. and Gold,L. (1982) Autoregulation of gene expression. Quantitative evaluation of the expression and function of the bacteriophage T4 gene 32 (single-stranded DNA binding) protein system. *J. Mol. Biol.*, **162**, 795–818.
9. Lohman,T.M. and Ferrari,M.E. (1994) Escherichia coli single-stranded DNA-binding protein: multiple DNA-binding modes and cooperativities. *Annual r. Rev. Biochem.*, **63**, 527–570.
10. Karpel,R.L. (1990) T4 bacteriophage gene 32 protein. In: Revzin,A (ed). *The Biology of Nonspecific DNA-Protein Interactions*. CRC Press, Boca Raton, FL, pp. 103–130.
11. Theobald,D.L., Mitton-Fry,R.M. and Wuttke,D.S. (2003) Nucleic acid recognition by OB-fold proteins. *Annu. Rev. Biophys. Biomol. Struct.*, **32**, 115–133.
12. Shamoo,Y., Friedman,A.M., Parsons,M.R., Konigsberg,W.H. and Steitz,T.A. (1995) Crystal structure of a replication fork single-stranded DNA binding protein (T4 gp32) complexed to DNA. *Nature*, **376**, 362–366.
13. Casas-Finet,J.R., Fischer,K.R. and Karpel,R.L. (1992) Structural basis for the nucleic acid binding cooperativity of bacteriophage T4 gene 32 protein: the (Lys/Arg)3(Ser/Thr)2 (LAST) motif. *Proc. Natl. Acad. Sci. U.S.A.*, **89**, 1050–1054.
14. Lonberg,N., Kowalczykowski,S.C., Paul,L.S. and von Hippel,P.H. (1981) Interactions of bacteriophage T4-coded gene 32 protein with nucleic acids. III. Binding properties of two specific proteolytic digestion products of the protein (G32P*I and G32P*III). *J. Mol. Biol.*, **145**, 123–138.
15. Kowalczykowski,S.C., Lonberg,N., Newport,J.W. and von Hippel,P.H. (1981) Interactions of bacteriophage T4-coded gene 32 protein with nucleic acids. I. Characterization of the binding interactions. *J. Mol. Biol.*, **145**, 75–104.
16. Lohman,T.M. and Kowalczykowski,S.C. (1981) Kinetics and mechanism of the association of the bacteriophage T4 gene 32 (helix destabilizing) protein with single-stranded nucleic acids. Evidence for protein translocation. *J. Mol. Biol.*, **152**, 67–109.
17. Newport,J.W., Lonberg,N., Kowalczykowski,S.C. and von Hippel,P.H. (1981) Interactions of bacteriophage T4-coded gene 32 protein with nucleic acids. II. Specificity of binding to DNA and RNA. *J. Mol. Biol.*, **145**, 105–121.

18. Pant,K., Karpel,R.L., Rouzina,I. and Williams,M.C. (2004) Mechanical measurement of single-molecule binding rates: kinetics of DNA helix-destabilization by T4 gene 32 protein. *J. Mol. Biol.*, **336**, 851–870.
19. Pant,K., Karpel,R.L., Rouzina,I. and Williams,M.C. (2005) Salt dependent binding of T4 gene 32 protein to single and double-stranded DNA: single molecule force spectroscopy measurements. *J. Mol. Biol.*, **349**, 317–330.
20. Pant,K., Karpel,R.L. and Williams,M.C. (2003) Kinetic regulation of single DNA molecule denaturation by T4 gene 32 protein structural domains. *J. Mol. Biol.*, **327**, 571–578.
21. Rouzina,I., Pant,K., Karpel,R.L. and Williams,M.C. (2005) Theory of electrostatically regulated binding of T4 gene 32 protein to single- and double-stranded DNA. *Biophys. J.*, **89**, 1941–1956.
22. Kelly,R.C., Jensen,D.E. and von Hippel,P.H. (1976) DNA 'melting' proteins. IV. Fluorescence measurements of binding parameters for bacteriophage T4 gene 32-protein to mono-, oligo-, and polynucleotides. *J. Biol. Chem.*, **251**, 7240–7250.
23. Jensen,D.E., Kelly,R.C. and von Hippel,P.H. (1976) DNA 'melting' proteins. II. Effects of bacteriophage T4 gene 32-protein binding on the conformation and stability of nucleic acid structures. *J. Biol. Chem.*, **251**, 7215–7228.
24. McGhee,J.D. and von Hippel,P.H. (1974) Theoretical aspects of DNA-protein interactions: co-operative and non-co-operative binding of large ligands to a one-dimensional homogeneous lattice. *J. Mol. Biol.*, **86**, 469–489.
25. Jose,D., Weitzel,S.E., Baase,W.A., Michael,M.M. and von Hippel,P.H. (2015) Mapping the interactions of the single-stranded DNA binding protein of bacteriophage T4 (gp32) with DNA lattices at single nucleotide resolution: Polynucleotide binding and cooperativity. *Nucleic Acids Res.*, doi:10.1093/nar/gkv818.
26. Delius,H., Mantell,N.J. and Alberts,B. (1972) Characterization by electron microscopy of the complex formed between T4 bacteriophage gene 32-protein and DNA. *J. Mol. Biol.*, **67**, 341–350.
27. van Amerongen,H., Kuil,M.E., Scheerhagen,M.A. and van Grondelle,R. (1990) Structure calculations for single-stranded DNA complexed with the single-stranded DNA binding protein GP32 of bacteriophage T4: a remarkable DNA structure. *Biochemistry*, **29**, 5619–5625.
28. Kelly,R.C. and von Hippel,P.H. (1976) DNA 'melting' proteins. III. Fluorescence 'mapping' of the nucleic acid binding site of bacteriophage T4 gene 32-protein. *J. Biol. Chem.*, **251**, 7229–7239.
29. Jose,D., Datta,K., Johnson,N.P. and von Hippel,P.H. (2009) Spectroscopic studies of position-specific DNA 'breathing' fluctuations at replication forks and primer-template junctions. *Proc. Natl. Acad. Sci. U.S.A.*, **106**, 4231–4236.
30. Johnson,N.P., Baase,W.A. and von Hippel,P.H. (2004) Low-energy circular dichroism of 2-aminopurine dinucleotide as a probe of local conformation of DNA and RNA. *Proc. Natl. Acad. Sci. U.S.A.*, **101**, 3426–3431.
31. Datta,K. and von Hippel,P.H. (2008) Direct spectroscopic study of reconstituted transcription complexes reveals that intrinsic termination is driven primarily by thermodynamic destabilization of the nucleic acid framework. *J. Biol. Chem.*, **283**, 3537–3549.
32. Jose,D., Weitzel,S.E. and von Hippel,P.H. (2012) Breathing fluctuations in position-specific DNA base pairs are involved in regulating helicase movement into the replication fork. *Proc. Natl. Acad. Sci. U.S.A.*, **109**, 14428–14433.
33. Bittner,M., Burke,R.L. and Alberts,B.M. (1979) Purification of the T4 gene 32 protein free from detectable deoxyribonuclease activities. *J. Biol. Chem.*, **254**, 9565–9572.
34. Mc,M.T. and Marshall,K. (1952) Specific volumes of proteins and the relationship to their amino acid contents. *Science*, **116**, 142–143.
35. Dam,J. and Schuck,P. (2005) Sedimentation velocity analysis of heterogeneous protein-protein interactions: sedimentation coefficient distributions c(s) and asymptotic boundary profiles from Gilbert-Jenkins theory. *Biophys. J.*, **89**, 651–666.
36. Dam,J., Velikovsky,C.A., Mariuzza,R.A., Urbanke,C. and Schuck,P. (2005) Sedimentation velocity analysis of heterogeneous protein-protein interactions: Lamm equation modeling and sedimentation coefficient distributions c(s). *Biophys. J.*, **89**, 619–634.
37. Schuck,P. (2000) Size-distribution analysis of macromolecules by sedimentation velocity ultracentrifugation and Lamm equation modeling. *Biophys. J.*, **78**, 1606–1619.
38. Williams,K.R. and Konigsberg,W. (1978) Structural changes in the T4 gene 32 protein induced by DNA polynucleotides. *J. Biol. Chem.*, **253**, 2463–2470.
39. Nordlund,T.M., Andersson,S., Nilsson,L., Rigler,R., Graslund,A. and McLaughlin,L.W. (1989) Structure and dynamics of a fluorescent DNA oligomer containing the EcoRI recognition sequence: fluorescence, molecular dynamics, and NMR studies. *Biochemistry*, **28**, 9095–9103.
40. Guest,C.R., Hochstrasser,R.A., Sowers,L.C. and Millar,D.P. (1991) Dynamics of mismatched base pairs in DNA. *Biochemistry*, **30**, 3271–3279.
41. Ballin,J.D., Prevas,J.P., Bharill,S., Gryczynski,I., Gryczynski,Z. and Wilson,G.M. (2008) Local RNA conformational dynamics revealed by 2-aminopurine solvent accessibility. *Biochemistry*, **47**, 7043–7052.
42. Kim,C. and Wold,M.S. (1995) Recombinant human replication protein A binds to polynucleotides with low cooperativity. *Biochemistry*, **34**, 2058–2064.
43. Sinha,N.K., Morris,C.F. and Alberts,B.M. (1980) Efficient in vitro replication of double-stranded DNA templates by a purified T4 bacteriophage replication system. *J. Biol. Chem.*, **255**, 4290–4293.
44. Draper,D.E. and von Hippel,P.H. (1978) Nucleic acid binding properties of Escherichia coli ribosomal protein S1. II. Co-operativity and specificity of binding site II. *J. Mol. Biol.*, **122**, 339–359.
45. Draper,D.E. and von Hippel,P.H. (1978) Nucleic acid binding properties of Escherichia coli ribosomal protein S1. I. Structure and interactions of binding site I. *J. Mol. Biol.*, **122**, 321–338.
46. Cantor,C.R. and Schimmel,P.R. (1980) *Biophysical chemistry*. W. H. Freeman, San Francisco.